

Journal of Biomedical Optics

SPIEDigitalLibrary.org/jbo

Reflection-mode time-reversed ultrasonically encoded optical focusing into turbid media

Puxiang Lai
Xiao Xu
Honglin Liu
Yuta Suzuki
Lihong V. Wang

Reflection-mode time-reversed ultrasonically encoded optical focusing into turbid media

Puxiang Lai, Xiao Xu, Honglin Liu, Yuta Suzuki, and Lihong V. Wang

Washington University in St. Louis, Department of Biomedical Engineering, Optical Imaging Laboratory, Campus Box 1097, 1 Brookings Drive, St. Louis, Missouri 63130

Abstract. Time-reversed ultrasonically encoded (TRUE) optical focusing was recently proposed to deliver light dynamically to a tight region inside a scattering medium. In this letter, we report the first development of a reflection-mode TRUE optical focusing system. A high numerical aperture light guide is used to transmit the diffusely reflected light from a turbid medium to a phase-conjugate mirror (PCM), which is sensitive only to the ultrasound-tagged light. From the PCM, a phase conjugated wavefront of the tagged light is generated and conveyed by the same light guide back to the turbid medium, subsequently converging to the ultrasonic focal zone. We present experimental results from this system, which has the ability to focus light in a highly scattering medium with a round-trip optical penetration thickness (extinction coefficient multiplied by round-trip depth) as large as 160. © 2011 Society of Photo-Optical Instrumentation Engineers (SPIE). [DOI: 10.1117/1.3609001]

Keywords: optical imaging; optical focusing; optical phase conjugation; ultrasonic modulation; time reversal; photorefractive crystal; turbid media; reflection mode.

Paper 11206LR received Apr. 25, 2011; revised manuscript received Jun. 16, 2011; accepted for publication Jun. 17, 2011; published online Aug. 11, 2011.

In soft biological tissue, photons undergo multiple scattering events and follow “random walks,” which result in a diffusive optical field with compromised spatial resolution for imaging purposes beyond one transport mean free path length (~ 1 mm). Hence, the problem of how to effectively focus or deliver light tightly deep into biological tissues has been of particular interest to the optical imaging community. Various schemes, such as adaptive wavefront shaping,¹ and optical phase conjugation,² have been developed to tackle this challenge. These techniques, however, require either time-consuming optimization¹ or focusing light through a turbid medium instead of inside it.²

Most recently, a new technique called time-reversed ultrasonically encoded (TRUE) optical focusing³ has been proposed to dynamically focus light to a small volume defined by a focused ultrasound wave inside a turbid medium regardless of the medium’s optical homogeneity. In this technique, photons are multiply scattered inside the experimental sample, the

ultrasound (US) wave modulates the propagation of those photons traveling through the region where light and sound coexist, i.e., the acousto-optic (AO) interaction volume,⁴ and tags photons with an ultrasonic frequency shift. Once the tagged photons (S) have diffused through the sample, they are collected by a photorefractive crystal (PRC), and interfere with a reference coherent optical beam (R) there to form a stationary hologram. The hologram is then read by a conjugated optical beam (R^*), resulting in a time-reversed wavefront (S^*). S^* tracks the same trajectories of S in the reversed directions, and converges back to the AO interaction volume. US focusing enables the AO interaction volume to be much smaller than the broad light distribution inside the turbid medium, achieving good focusing. The feasibility of TRUE optical focusing has been demonstrated³ and further characterized in tissue-mimicking phantoms with optical focusing thicknesses (product of optical extinction coefficient and sample thickness) up to 70.⁵

The experimental setup implemented in Refs. 3 and 5 employs a transillumination configuration where optical incidence and collection are on opposite sides of an experimental sample. Such an alignment may pose limitations on applications in medical imaging where transmitting illumination leads to an undesirable increase in operative optical penetration. To make this new technique more practical and convenient, a reflection-mode TRUE optical focusing system has been developed, in which the optical input and output modules are installed on the same side of a sample, as reported in this letter.

Figure 1(a) is a schematic depiction of the experimental apparatus. The time sequences of holographic writing and reading, US modulation, and unveiling of the photodiode (by S_5) within each system cycle are shown in Fig. 1(b). A continuous-wave laser (Verdi V-10, Coherent) operating at 532 nm was the light source. Its output was split into a sample beam (S), a reference beam (R), and a reading beam (R^*). During the first 190 ms of each cycle, R^* was blocked, and two acousto-optic modulators (AOMs, 802AF1, IntraAction) were employed in combination to tune the sample beam frequency from f_0 to $f_0 - f_a$, where f_0 represents the frequency of the laser and f_a the net frequency shift due to the AOMs. The resulting sample beam was expanded and directed along the Y direction to illuminate the front surface of the experimental sample with an approximate optical intensity of 880 mW/cm². Unless otherwise mentioned, porcine gelatin (Sigma) gel-based phantoms doped with intralipid (Fresenius Kabi) ($\mu'_s = 20$ cm⁻¹) were used as optical tissue-mimicking samples in the study. Within the sample, light was multiply scattered and phase modulated by the applied focused ultrasonic waves at a frequency of f_a . The resultant backscattered light, composed of three spectral components at $f_0 - f_a$, $f_0 - 2f_a$, as well as f_0 , was collected from the same side of the sample by an obliquely and closely mounted fiber optical light guide (NT 39-370, Edmund Optics) that had a high optical etendue, as illustrated in Fig. 1(a). In a $10 \times 10 \times 5$ mm³ Bi₁₂SiO₂₀ (BSO) crystal (Elan, Russia), the collected signal light interfered with R (30 mW/cm²) at an angle of ~ 13.6 deg. Note that only the interference between $S(f_0)$ and R at the same frequency f_0 could form a stationary hologram inside the crystal.⁶ To enhance the holographic recording efficiency, a 2.1 kHz, 8 kV/cm

Address all correspondence to: Lihong V. Wang, Washington University in St. Louis, Department of Biomedical Engineering, Optical Imaging Laboratory, Campus Box 1097, 1 Brookings Drive, St. Louis, Missouri 63130; Tel: (314) 935-6152; Fax: (314) 935-7448; E-mail: lhwang@biomed.wustl.edu.

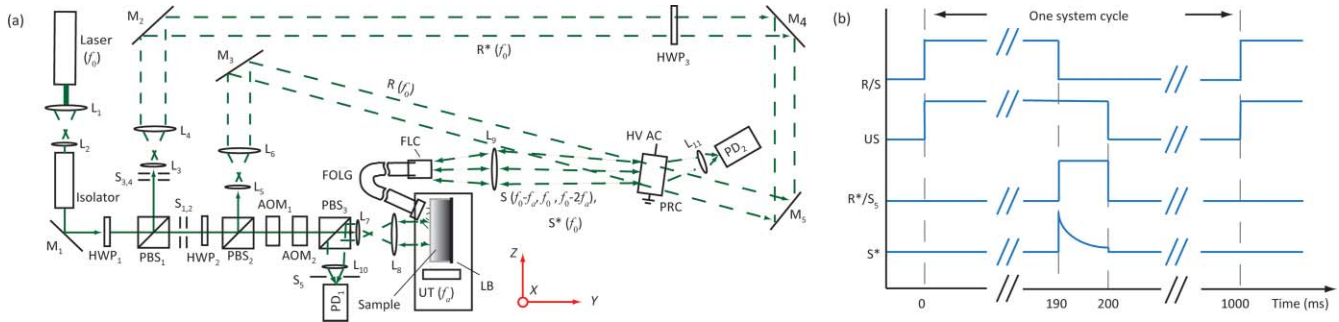


Fig. 1 (a) Experimental schematic of the reflection-mode TRUE optical focusing system. The component labels are defined as follows: f_0 , frequency of laser; f_a , frequency of ultrasound; L_1-11 , lenses; M_1-5 , mirrors; HWP_{1-3} , half-wave plates; PBS_{1-3} , polarizing beam splitters; S_{1-5} , shutters; $AOM_{1,2}$, acousto-optic modulators; $PD_{1,2}$, photodiodes; UT, ultrasound transducer; LB, light block; FOLG, fiber optical light guide; FLC, fiber light condenser; PRC, photorefractive crystal; HV ac, high-voltage ac electric field applied across the PRC; S , reflectively collected diffused light from the sample; R , reference beam; R^* , conjugate reference beam; S^* , time-reversed copy of S ; XYZ , system coordinates (Y is the optical illumination direction, and Z is the US propagation axis). (b) Temporal sequences within one system cycle (1 s).

(peak-to-peak) high voltage (square) ac electric field from an amplifier (609E-6-L-CE, Trek) was applied across the crystal.

In the subsequent reading phase, when S and R were blocked by the shutters $S_{1,2}$, R^* (~ 900 mW/cm²) illuminated the crystal along the direction opposite to R , and instantly generated a phase conjugated copy of $S(f_0)$, namely $S^*(f_0)$. The copy followed the exact trajectories of $S(f_0)$ back into the medium to converge to the US focal volume, thereby accomplishing optical focusing inside the turbid medium. Part of this time-reversed, locally concentrated light was again backscattered, then collected in the reflection configuration by a photodiode detector (PD_1 , PDA36A, Thorlabs) outside of the sample.

Figure 2 shows examples of signal waveforms (8 times averaging) reaching PD_1 from a highly scattering medium. As we can see, even though $S_{3,4}$ were triggered to launch at time 190 ms [Fig. 1(b)], due to the shutter response delay and finite operating speed, no light entered PD_1 until approximately 191.5 ms. In the case of no US modulation, no time-reversed signal was generated. Therefore only some randomly scattered reading beam from the PRC arrived at PD_1 , giving a relatively flat background before R^* and S_5 were shut off at 201.5 ms.

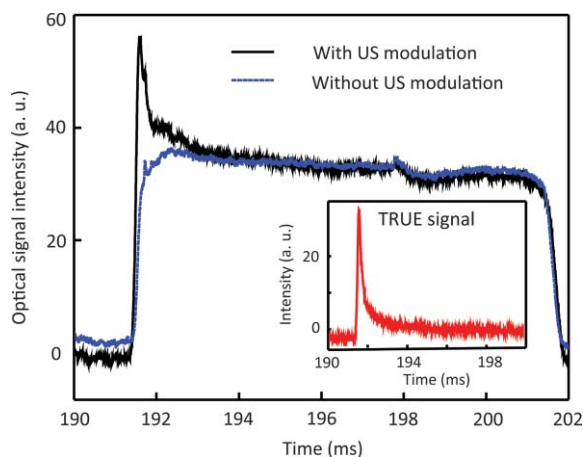


Fig. 2 Examples of time-domain optical signals reaching PD_1 from a highly scattering medium with and without US modulation. Their subtraction gives the TRUE signal shown in the inset.

With US modulation, however, S^* was generated immediately after R^* was allowed to pass [by $S_{3,4}$ in Fig. 1(a)] rendering a sharp peak standing above the background. The difference between these two PD_1 signals, shown in the inset, provides the TRUE optical response, whose peak value is defined as the TRUE signal intensity in the study.

Since the US modulation depth is related to the local optical properties within the US focus,⁷ so are the consequent hologram contrast and TRUE signal intensity. Therefore, the TRUE signal intensity can be used to gauge the efficacy of optical focusing in turbid media. To validate this experimentally, a single-element focused transducer (A381S, Olympus) that had a central frequency at 3.5 MHz and a full-width at half maximum (FWHM) of 0.87 mm at focus was used as the US modulation source. In our study, focal pressures at 1.0 MPa (peak-to-peak) were used. The US propagation axis was aligned perpendicular to the incident sample beam, so that the focal point intersected with the center of the laser beam. A 6-mm thick highly scattering layer ($\mu_a \approx 0.08$ cm⁻¹, $\mu'_s = 20$ cm⁻¹) was prepared as shown in Fig. 3(a) and sandwiched between two transparent gelatin gels along the Y direction for better acoustic coupling. The sample beam S was incident from the left, and $Y = 0$ was set to the front (left) boundary of the scattering layer. On the XZ plane around $Y = 2$ mm, i.e., 2 mm deep in the turbid medium, three absorption inclusions were embedded as illustrated in Fig. 3(b). These inclusions, with dimensions of $1 \times 1 \times 8$ to 10 mm³ along the XYZ axes and separated by 4.5 to 4.8 mm along the X axis, were made of the same material as the turbid background, except that India ink was added to provide optical absorption contrast against the background: $\mu_a = 1$ cm⁻¹ for Obj 2, and 0.4 cm⁻¹ for Obj 1 and 3.

In the experiments, the transducer was first moved along the Y direction to position the US focal point 2 mm deep in the scattering layer (the same Y plane where the inclusions were embedded). Both the light and the ultrasound were kept stationary, while the phantom was scanned along the X direction with a step size of 0.127 mm. At each position, a TRUE signal was obtained as discussed in Fig. 2. A dc signal and a time-reversed direct current (TRDC) signal were also recorded at PD_2 and PD_1 , respectively, when the AOM tuning and US modulation were turned off. The result of the scan is shown in Fig. 3(c),

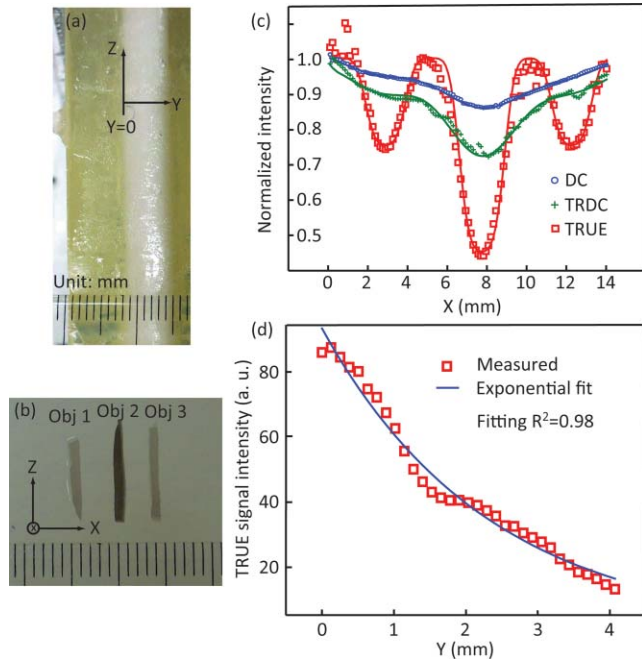


Fig. 3 (a) Photograph of the phantom in the YZ plane, showing the 6-mm thick scattering layer sandwiched between transparent gel layers. (b) Phantom cross-section in the XZ plane at $Y = 2$ mm, showing three embedded absorbing targets. (c) Normalized dc, TRDC, and TRUE signal intensity distribution along the X direction. (d) TRUE signal intensity as a function of US focal position along the Y direction.

where the normalized signal intensities are plotted as a function of X . The dc and TRDC images have spatial resolutions of 3.3 and 2.8 mm, respectively, based on the FWHM of their Gaussian fits,³ and thus lack the ability to resolve the three objects due to the light diffusion. For TRUE, however, the embedded objects are evident against the background. Their fitted widths, based on the Gaussian fit, measure 1.0, 1.1, and 1.0 mm, respectively, agreeing well with the actual widths of the objects. Spacings between the adjacent objects are also consistent with the actual positions. In addition, Obj 2 produced a lower TRUE signal intensity than the other two targets due to its higher absorption coefficient, suggesting less light was focused back to the US focus at Obj 2's position. Finally, the spatial resolution of the TRUE image, computed from the FWHM of the Gaussian fit, was 0.63 mm, which is approximately $1/\sqrt{2}$ of the US focal width and consistent with the square law.³ All of these findings lead us to conclude, although indirectly, that the reflection-mode TRUE focusing system was able to focus light back to the US focal zone within a turbid medium.

Figure 3(d) shows the TRUE signal intensity as a function of US focus depth in the sandwiched turbid layer. Measurements were performed by scanning the transducer along the Y direction, with the US focus away from the three objects in the X direction, while the phantom and the optical incidence/collection were kept fixed during the scan. From Fig. 3 we can see that the measured TRUE signal intensity (squares) decays approximately exponentially when the US beam moves deeper into the scattering layer and fits quite well with a model (curve, the fitting coefficient of determination $R^2 = 0.98$) $Y = 92.92 \cdot \exp(-0.432 \cdot d)$, where d is the Y position of the US focus in millimeters. Considering

that light was collected in a reflection configuration, the actual optical depth for penetration was $2d$. Therefore, the TRUE signal intensity had an exponential decay rate of $0.432/2 = 0.215 \text{ mm}^{-1}$, close to the effective attenuation coefficient of the medium ($\mu_{\text{eff}} = \sqrt{3\mu_a(\mu_a + \mu_s')} \approx 0.219 \text{ mm}^{-1}$) that governs the decay of fluence rate for diffused light. It should be noted that the measured values deviate more from the fitted results at depths around 2 mm, which may be due to the slight mismatch in acoustic impedance and index of refraction since the layers of turbid media on the right and on the left of the $Y = 2$ mm plane were solidified separately in the process of phantom fabrication to embed the three absorption objects. Nevertheless, the overall consistency once again validates that TRUE optical focusing converged diffused light tightly back to the US focus and created a virtual light source within the turbid media. The maximum focusing depth with our current setup, as shown here, is more than 4 mm into such a highly scattering medium. The round-trip optical penetration thickness of $(\mu_a + \mu_s) \times 2d \approx 160$ is equivalent to 16 mm in tissue-mimicking phantoms that have an optical extinction coefficient of 10 mm^{-1} .

In summary, this letter presents the development of the first reflection-mode TRUE optical focusing system, with demonstrated the ability to dynamically focus diffused light into a tight volume guided by ultrasound focus within turbid media. Compared with previous schemes in transmission mode, the reported reflection-mode configuration using a light guide for back-scattered diffused light collection and transition is more convenient and practical, and a round-trip optical penetration thickness as much as 160 was reached. As a new technique, TRUE optical focusing is not mature yet. However, further improvements, especially with regard to penetration depth and time-reversed signal gain, together with tests in tissues, will undoubtedly make this innovation more attractive.⁸

Acknowledgments

The authors thank Professor James Ballard for editing the manuscript. This research is sponsored in part by the NIH through Grants R01 EB000712 and U54 CA136398.

References

1. I. M. Vellekoop, E. G. van Putten, A. Lagendijk, and A. P. Mosk, "Demixing light paths inside disordered metamaterials," *Opt. Express* **16**, 67–80 (2008).
2. Z. Yaqoob, D. Psaltis, M. S. Feld, and C. Yang, "Optical phase conjugation for turbidity suppression in biological samples," *Nature Photonics* **2**, 110–115 (2008).
3. X. Xu, H. Liu, and L. V. Wang, "Time-reversed ultrasonically encoded optical focusing into scattering media," *Nature Photonics* **5**, 154–157 (2011).
4. L. V. Wang, "Mechanisms of ultrasound modulation of multiply scattered coherent light: An analytic model," *Phys. Rev. Lett.* **87**, 043903 (2001).
5. H. Liu, X. Xu, P. Lai, and L. V. Wang, "Time-reversed ultrasonically encoded (TRUE) optical focusing into tissue-mimicking media with thickness up to 70 mean free paths," *J. Biomed. Opt.* **16**, 086009 (2011).
6. L. Solymar, D. J. Webb, and A. G. Jepsen, *The Physics and Applications of Photorefractive Materials*, Clarendon Press, Oxford (1996).
7. P. Lai, R. A. Roy, and T. W. Murray, "Quantitative characterization of turbid medium using pressure contrast acousto-optic imaging," *Opt. Lett.* **34**, 2850–2852 (2009).
8. S. D. Konecky and B. J. Tromberg, "Focusing light in scattering media," *Nature Photon.* **5**, 135–136 (2011).